Published in "Chinese Physics Letters 34(5): 058501, 2017"
which should be cited to refer to this work.

All-Optical Vector Cesium Magnetometer *

Wei-Min Sun(孙伟民)[1,2], Qiang Huang(黄强)[1,2], Zong-Jun Huang(黄宗军)[2],
Ping-Wen Wang(王平稳)[2], Jun-Hai Zhang(张军海)[2,3]**

[1] *College of Automation, Harbin Engineering University, Harbin 150001*
[2] *Key Lab of In-fiber Integrated Optics (Ministry Education), Harbin Engineering University, Harbin 150001*
[3] *Physics Department, University of Fribourg, Fribourg 1700, Switzerland*

Based on power modulation of a pump laser and precessional projection detection, we present an all-optical vector magnetometer of cesium, which has a demonstrated magnitude sensitivity of 80 fT/Hz$^{1/2}$ and an orientation sensitivity of 0.1°/Hz$^{1/2}$. In the device, four main factors are measured experimentally, which are the Larmor precession frequency of a polarized magnetic moment that depends on the modulus of the measured magnetic field only, two phase shifts and amplitude ratio of the precession projection in the two probe directions relative to the magnetic field orientation. This kind of magnetometer with high sensitivity in the range of the spatial angle is suitable for solving the inverse problem and geomagnetic navigation.

As the most sensitive devices for measuring magnetic fields,[1] the atomic spin-precession magnetometer has two fundamental kinds according to differences of the measurement parameters of the magnetic field. One is the scalar magnetometer that gives only the magnetic field magnitude by measuring the Larmor frequency of polarized atoms directly or indirectly. It may be applied in the field of measuring magnetic field fluctuation in the specified direction, for example, nuclear magnetic resonance,[2–5] and biological medical imagining.[6,7] The other is the vectorial magnetometer that can record all information of the field, thus it plays an essential role in geophysical measurement, spatial navigation and planetary observation.[8–10] There are several main approaches to realize atomic vector measurement from a scalar magnetometer. By compensating for the magnetic field measured, the scalar magnetometer is kept operating near zero field,[11,12] where the sensitivity greatly depends on the noise level of compensation of the magnetic field. It is also possible to extract orientation information of the magnetic field by means of the dependence of electromagnetically induced transparency (EIT) on the magnetic direction in a linearly polarized bi- or polychromatic light configuration.[13,14] In the case of the existence of an offset field in one direction, using magnetic modulation and demodulation in the other two orthogonal directions, the vector components of a weak measured field can be obtained,[15,16] because here the outputs of the lock-in amplifier are proportional to the components of the field in corresponding directions. Furthermore, to overcome a possibly suffered disturbance of a weak oscillating magnetic field driving the Zeeman transition to magnetic field measured, Bell *et al.* discovered that circularly polarized light with power modulation could induce atomic magnetic resonance in the ground state.[17] Recently, modulation technology of the all-optical parameters (including amplitude, frequency, and polarization) has been developed rapidly.[18–21] The advantage of this technology has been mainly shown on avoiding the influence of metal components near atom sensor and signal crosstalk in a magnetometer array.[22] However, few investigations have been carried out on the all-optical vector magnetometer having better than 500 fT/Hz$^{1/2}$ sensitivity without bias magnetic field.

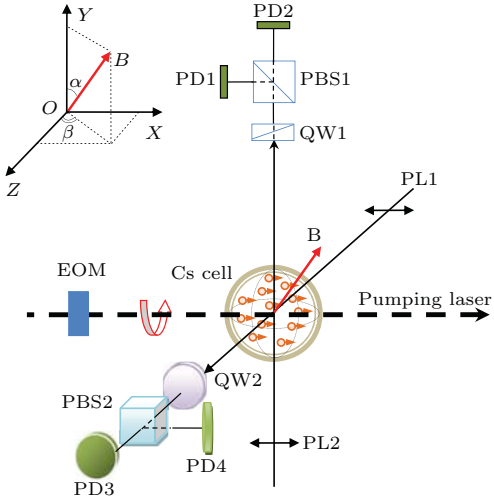

Fig. 1. Principle of the all-optical vector magnetometer. EOM: electro-optic modulator, QW: quarter-wave, PL: probe laser, and PD: photo detector.

In this Letter, we report on an all-optical vector magnetometer with three orthogonal laser beams, which can synchronously track the precession caused by the measured magnetic vector. It is able to read out the modulus of the magnetic field through the resonant frequency and to determine the field orientation by means of the phase of precession projection in

*Supported by the National Natural Science Foundation of China under Grant Nos U1631239 and U1331114, and the 111 Project to Harbin Engineering University under Grant No B13015.
**Corresponding author. Email: jhzhang@hrbeu.edu.cn

two probe beam directions and their amplitude ratios. Using pumping modulation and amplitude projection detection of the precession, the experiment demonstrates that the magnetometer not only has the optimum magnitude sensitivity of $80\,\mathrm{fT/Hz^{1/2}}$ and the orientation sensitivity of $0.1^\circ/\mathrm{Hz^{1/2}}$, but also can keep the sensitivity better than $120\,\mathrm{fT/Hz^{1/2}}$ in the range of large spatial angle. This type of magnetometer is more appropriate for positioning and navigating.

The principle of the magnetometer is sketched in Fig. 1. The cesium vapor can be polarized by a resonance laser with circular polarization and an initial magnetic moment is immediately generated along the pumping x direction. If there is a magnetic vector measured, it should induce the moment to precess around the vector, and the time-dependent solution of the moment would be written by the Bloch equation[12,21]

$$P'(t) = \gamma B \times P(t) - \Gamma P(t) + P_0(t)i, \qquad (1)$$

where $P(t)$ is the magnetic moment vector, $\gamma = 2\pi \times 3.5\,\mathrm{Hz/nT}$ is the gyromagnetic ratio of Cs, $B(|B|, \alpha, \beta)$ represents the magnetic vector measured by us and the corresponding Larmor frequency $\omega_\mathrm{L} = \gamma|B|$ (α is the angle between the magnetic vector and the y axis, and β is the angle between the z axis and the projection of the vector in the $y = 0$ plane), and Γ is the transverse relaxation rate of the precession. The last term in Eq. (1) describes the effect of the pumping laser to polarize atoms along x, which is given by[21]

$$P_0(t) = \frac{R_\mathrm{op} S_0}{2}[1 + \cos(\omega t)], \qquad (2)$$

where R_op and S_0 are the optical pumping rate and the magnetic moment induced by the unit pumping rate in zero magnetic intensity, respectively, and ω represents the modulation frequency of the pumping laser near ω_L. Two linear polarization lights propagating along the z and y axes are used to detect the precessional projections in the corresponding directions.

To analyze the information of the precession projection in the z and y directions, we need to make three assumptions: (1) $\omega_\mathrm{L} \gg \Gamma \gg 1$, (2) the influence of longitudinal relaxation on the precession is not taken into account under the condition of varying field orientation, and (3) the counter-propagating rotational response at $-\omega$ is ignored. Then the time dependence of precession components in three coordinate axes may be expressed as[23]

$$P_x(t) = \Gamma R_\mathrm{op} S_0 \frac{A_x(\alpha,\beta)}{\sqrt{\Gamma^2 + (\omega - \omega_\mathrm{L})^2}} \cdot [\cos(\omega t) - 1] + \frac{R_\mathrm{op} S_0}{2\Gamma}, \qquad (3)$$

$$P_i(t) = \Gamma R_\mathrm{op} S_0 \frac{A_i(\alpha,\beta)}{\sqrt{\Gamma^2 + (\omega - \omega_\mathrm{L})^2}} \cdot [\cos(\omega t - \varphi_i) - \cos(\varphi_i)], \qquad (4)$$

where $i = z$ or y, $A_x(\alpha, \beta)$ and $A_i(\alpha, \beta)$ are proportional to the amplitude of precession's x and i direction projection, as a function of the field orientation, and ϕ_i represents the phase shift in the i direction assuming that the initial phase is zero in the x direction. Inserting Eqs. (3) and (4) into Eq. (1), the coefficients of harmonic components on both sides of the equation must be equal, and using Wolfram Mathematica 10.0, the above four parameters $A_y(\alpha, \beta)$, $A_z(\alpha, \beta)$, ϕ_y and ϕ_z we are interested in can be obtained numerically on resonance.

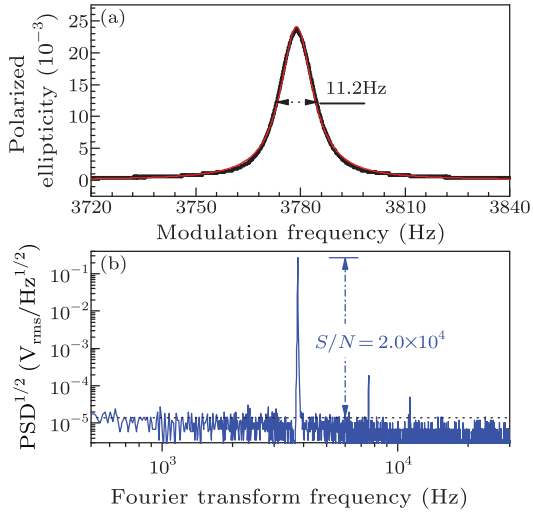

Fig. 2. (a) Projection amplitude of the precession versus the EOM modulation frequency. The black points represent the experimental data. The red curve is a Lorentzian fit. (b) Power spectrum density (PSD) of (a).

In our experimental setup, a spherical vapor cell with a 30 mm external diameter contains saturated cesium vapor and 70 Torr of helium that serves as the buffer gas to allow much lengthening interaction time and narrowing the spectral width effectively. The Cs metal is heated to 39℃ by flowing hot gas to obtain Cs vapor density of $2\times10^{11}\,\mathrm{cm^{-3}}$. The cell is magnet-shielded with cylinder permalloy shielding, which has 10^5 radial shielding factor and 2×10^4 axial factor because it is open on one side. The magnetic vector is created by a y-direction Helmholtz coil and a quasi Helmholtz coil, and the field yielded by the latter is located horizontally at the bisecting of angle $\angle xoz$, which means that the experimental fields have the identical $\beta = \pi/4$. Two current sources having short-term relative stability of 10^{-7} in 1 s provide electric current for both coils. Two external cavity laser diodes with 1 MHz line width are used. First, an σ^+ pump light with $8\,\mathrm{mm^2}$ cross section and 650 μW power is actively stabilized to the center of $F_\mathrm{g} = 3 \rightarrow F_\mathrm{e} = 4$ hyperfine transition of the cesium D_1 line by saturated absorption spectra. The pump intensity is modulated with an electro-optic modulator (EOM) by a square wave with 50% duty cycle near. The other linearly polarized probe laser is locked to the $F_\mathrm{g} = 4 \rightarrow F_\mathrm{e} = 5$ cycling transition of the cesium D_2 line. It is split into two beams propagating along the z and y directions, respectively, while each has $2\,\mathrm{mm^2}$ cross section and 2 μW power, and traverses through the polarized samples, a quarter-wave (QW) plate and a polarizing

beam splitter (PBS) in turn. The axis of the PBS is oriented at 45° with respect to the fast axis of the $\lambda/4$ plate. In this case, the measurement of ellipticity of linear polarization light could not be dependent on dispersion of the σ^+ and σ^- components, and that it may be expressed by $\xi \approx \frac{e^{-2\chi^+}-e^{-2\chi^-}}{e^{-2\chi^+}+e^{-2\chi^-}} \approx 10^{-2}$, where χ^+ and χ^- are the absorption parameters for both circular polarization components. Unlike ordinary polarization rotation detection where the probe frequency has to be controlled to a largely detuning position,[24,25] the ellipticity detection simply needs the frequency to be locked resonantly. In addition, the photodiodes of balanced amplified photo detectors (PD) record the precessional projections along y and z, and a dual-phase lock-in amplifier (LIA) allows the measurement of the amplitude and phase of the projections at each beam.

There is evidence that the magnetometer may have an optimum magnitude sensitivity of $80\,\mathrm{fT/Hz^{1/2}}$. When the field along the y axis (i.e., $\alpha = 0°$) has $1.08\,\mu\mathrm{T}$ magnitude, experiments measured the projection amplitude of the precession in the z axis, as a function of the modulation frequency of pumping light is shown in Fig. 2(a). Experimental data were fitted with an absorptive Lorentzian function. The spectrum having a line width of 11.2 Hz implies 70 Torr helium buffer gas should be more suitable for increasing atomic coherence life at the temperature compared with 100 Torr in Ref. [26], because the buffer gas not only decreases collision of the polarized atoms with the internal wall of the cell, but also causes the Cs-He relaxation to increase. The square root of power spectrum density (PSD) of the resonant spectrum and the signal-to-noise ratio (SNR) of about 20000 are displayed in Fig. 2(b). In terms of the magnetometer's sensitivity proportional to spectral slope divided by the SNR,[27] we are able to certify the magnetometer with $80\,\mathrm{fT/Hz^{1/2}}$ noise equivalent magnetic field.

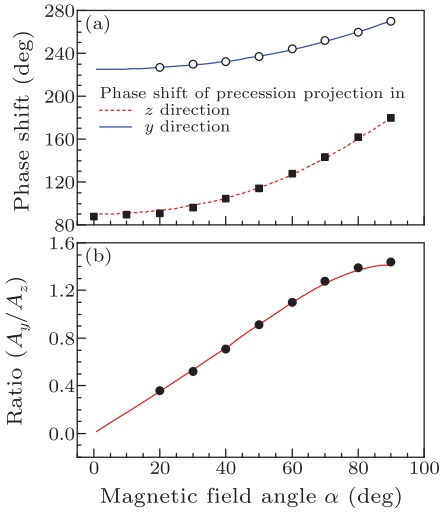

Fig. 3. (a) Phase changes of precession projection in the z and y directions as a function of the field direction. (b) Dependence of the amplitude ration on the field angle.

Then, we further discuss the influence of the field orientation on phase angle $\phi_{y(z)}$ of the projection in both probe directions and the ratio of their corresponding amplitudes, in the first octant (Fig. 1). In the experiment, all field orientation has the same $\beta = \pi/4$ and only a sole directional variable α. In the case of weak magnetic strength, the effect of nonlinear Zeeman shift on atomic precession can be neglected. Setting $1.08\,\mu\mathrm{T}$ amplitude of the field unchanged, we investigate the dependence of $\phi_{y(z)}$ on the orientation α in $y(z)$ (Fig. 3(a)) and the corresponding ratio of the amplitudes (Fig. 3(b)) simultaneously. In view of the small amplitude in the y axis at $\alpha = 10°$, the projection was recorded from $\alpha = 20°$ experimentally in the direction.

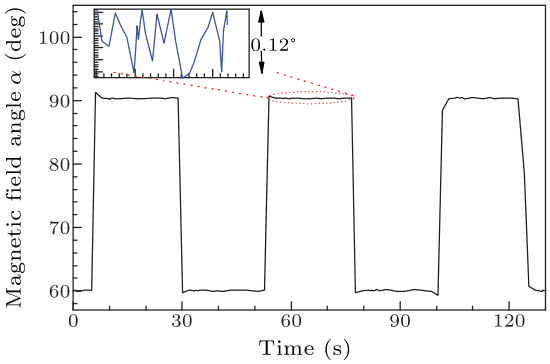

Fig. 4. Measurement for the field angle fluctuation in time domain. Inset: its magnification.

Here the red (blue) solid line of Fig. 3(a) is the theoretical curve in the $z(y)$ detection derived from Eq. (1), and closed (open) circles are experimental data in the corresponding directions. In Fig. 3(b), the red curve is derived from the above-mentioned calculation, i.e., the value of $A_y(\alpha,\beta)/A_z(\alpha,\beta)$ from Eq. (4), while the dots represent the measurement result. The pictures have shown perfectly the consistency between the experimental results and the proposed model, if the deviation of less than 2% from measurement environment fluctuation is taken into account, for instance, the variations from lasers' parameters and the field instability. Further, considering the field symmetry in space, we have reasonably confirmed that the field orientation should be determined by the phase variation and the ratio. To evaluate the uncertainty of the field angle, setting the field with constant intensity of $1.08\,\mu\mathrm{T}$ and switching at $\alpha = 60°$ and 90° at intervals, the angle fluctuation in Fig. 4 along the z axis was recorded. In view of the measurement bandwidth of 1.25 Hz, the magnetometer with $0.1°/\mathrm{Hz^{1/2}}$ direction sensitivity has been demonstrated.

We have also experimentally studied the magnitude sensitivity in the field with different magnetic orientations. Based on the fact that the magnetometer has the highest amplitude at $\alpha = 0°$ and the spectral noise is independent of the field orientation, we may then analyze a magnetometer's relative sensitivity which is defined as the ratio of the sensitivity with the orientation angle to the highest magnitude sensitivity, i.e., $\delta B_{\mathrm{rel}(i)} = \frac{\delta B_i}{80\,\mathrm{fT\cdot Hz^{-1/2}}}$ ($i = z$ or y),

where δB_i is the amplitude sensitivity in the i direction. Considering that the experiment detects the precessional projections in the z and y directions, one may estimate the whole relative amplitude sensitivity by $\delta B_{\mathrm{rel(whole)}} = [(\delta B_{\mathrm{rel}(z)})^{-2} + (\delta B_{\mathrm{rel}(y)})^{-2}]^{-1/2}$. Figure 5 illustrates the influence of the orientation on the relative sensitivity, the red (blue) curve is the relative sensitivity in the $z(y)$ detection theoretically and the black one corresponds to the whole relative amplitude sensitivity, while solid (open) squares, circles refer to the experimental points correspondingly. We estimate therein the whole relative sensitivity at $\alpha = 0,\ 10^\circ$ by means of the theoretical result in the y direction. The picture has shown that the amplitude sensitivity of the magnetometer is better than $120\,\mathrm{fT/Hz^{1/2}}$ in the angle range. It is found that the experimental deviation increases with α slowly, reaching the value of about 30% at $\alpha = 90^\circ$. The variation of deviation may be caused mainly by precessional spectral broadening and its reasons are analyzed as follows. Firstly, the contribution from longitudinal relaxation to the precession can be more significant with the increasing angle, whereas it is ignored in our model. Secondly, the broadening is caused by magnetic field gradients because of the imperfection of the measured field.[28] Lastly, the difference between axial and radical shielding factors of the shield cylinder might be another reason for affecting the spectral width. Consequently, making a perfect cell whose spectral width will not depend on the field orientation, i.e., the longitudinal relaxation rate is equal to the transverse rate,[29] is going to become a potential research subject. We have to point out that the dead zone and measurement range of the magnetometer are also important parameters, but they have been limited by our current source and coils arrangement for yielding the magnetic field, which are not researched in detail. Nevertheless, they will also still be a topic for future study.

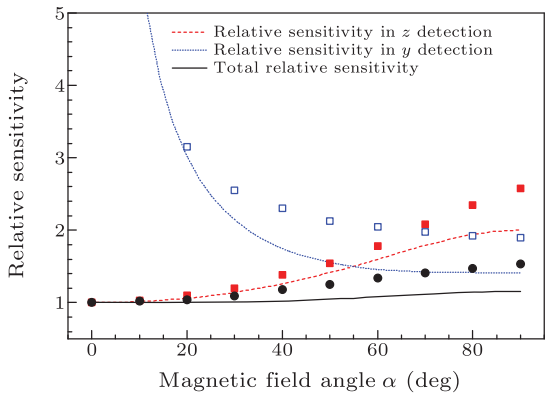

Fig. 5. Dependence of the relative sensitivity on the magnetic field direction in the magnetometer.

In summary, we have realized an all-optical vectorial magnetometer with the configuration of three orthogonal laser beams in a proof-of-principle experiment. Using power modulation of the pump laser and the detection of the precession projection, the magnetometer would have $80\,\mathrm{fT/Hz^{1/2}}$ magnitude sensitivity and $0.1^\circ/\mathrm{Hz^{1/2}}$ directional sensitivity. It is demonstrated experimentally that the Larmor frequency determines the field magnitude, and the phases of the precession projections in both the probe directions and the ratio of the two projection amplitudes determine the field orientation together. The variation of the magnitude sensitivity on the field orientation has also been discussed.

We thank Dr. Zoran Grujić for our useful discussion and critical reading of the manuscript.

References

[1] Budker D and Romalis M 2007 *Nat. Phys.* **3** 227
[2] Brown J M, Smullin S J, Kornack T W and Romalis M V 2010 *Phys. Rev. Lett.* **105** 151604
[3] Dang H B, Maloof A C and Romalis M V 2010 *Appl. Phys. Lett.* **97** 151110
[4] Shah V, Knappe S, Schwindt P D D and Kitching J 2007 *Nat. Photon.* **1** 649
[5] Savukov I, Karaulanov T and Boshier M G 2014 *Appl. Phys. Lett.* **104** 023504
[6] Lee H J, Shim J H, Moon H S and Kim K 2014 *Opt. Express* **22** 19887
[7] Xia H, Baranga B A, Hoffman D and Romalis M V 2006 *Appl. Phys. Lett.* **89** 211104
[8] Blogh A 2010 *Space Sci. Rev.* **152** 23
[9] Goldenberg F 2006 *IEEE/ION Position Location Navigation Symp.-PLANS* (San Diego California USA 25–27 April 2006) p 684
[10] Lenci L, Auyuanet A, Barreiro S, Valente P, Lezama and Failache H 2014 *Phys. Rev.* A **89** 043836
[11] Dong H F, Lin H B and Tang X B 2013 *IEEE Sens. J.* **13** 186
[12] Seltzer S J and Romalis M V 2004 *Appl. Phys. Lett.* **85** 4804
[13] Yudin V I, Taichenachev A V, Dudin Y O, Velichansky V L, Zibrov A S and Zibrov S A 2010 *Phys. Rev.* A **82** 033807
[14] Cox K, Yudin V I, Taichenachev A V, Novikova I and Mikhailov E E 2011 *Phys. Rev.* A **83** 015801
[15] Patton B, Zhivun E, Hovde D C and Budker D 2014 *Phys. Rev. Lett.* **113** 013001
[16] Vershovskii A K 2011 *Tech. Phys. Lett.* **37** 140
[17] Bell W E and Bloom A 1961 *Phys. Rev. Lett.* **6** 280
[18] Wang M L, Wang M B, Zhang G Y and Zhao K F 2016 *Chin. Phys.* B **25** 060701
[19] Huang H C, Dong H F, Hao H J and Hu X Y 2015 *Chin. Phys. Lett.* **32** 098503
[20] Acosta V, Ledbetter M P, Rochester S M, Budker D and Kimball D F J 2006 *Phys. Rev.* A **73** 053404
[21] Grujić Z D and Weis A 2013 *Phys. Rev.* A **88** 012508
[22] Grujić Z D, Koss P A, Bison G and Weis A 2015 *Eur. Phys. J.* D **69** 135
[23] Asaf G, Michael J H S and Subhas C M 2017 *High Sensitivity Magnetometers* (Switzerland: Springer) p 382
[24] Fang J C, Wan S A, Qin J, Zhang C and Quan W 2014 *J. Opt. Soc. Am.* B **31** 512
[25] Fu J Q, Du P C, Zhou Q and Wang R Q 2016 *Chin. Phys.* B **25** 010302
[26] Zhang J H, Liu Q, Zeng X J, Li J X and Sun W M 2012 *Chin. Phys. Lett.* **29** 068501
[27] Weis A, Bison G and Pazgalev A S 2006 *Phys. Rev.* A **74** 033401
[28] Pustelny S, Kimball D F J, Rochester S M, Yashchuk V V and Budker D 2006 *Phys. Rev.* A **74** 063406
[29] Bevilacqua G, Breschi E and Weis A 2014 *Phys. Rev.* A **89** 033406